Partial oxidation of methane to hydrogen and carbon monoxide over a Ni/TiO$_2$ catalyst

Tinghua Wu[a,*], Qiangu Yan[a,b,c], Huilin Wan[a,b]

[a] *Department of Chemistry, Institute of Physical Chemistry, Zhejiang Normal University, Zhejiang 321004, PR China*
[b] *The State Key Laboratory for Physical Chemistry of Solid Surface, Department of Chemistry,*
Xiamen University, Xiamen, Fujian 361005, PR China
[c] *Center for Advanced Vehicular Systems, Mississippi State University, Starkville, MS 39759, USA*

Abstract

Partial oxidation of methane to hydrogen and carbon monoxide (POM) over a Ni/TiO$_2$ catalyst has been investigated using a fixed-bed reactor. Ni/TiO$_2$ catalyst has high initial activity but undergoes deactivation during POM. Activation of methane on Ni/TiO$_2$ was studied by employing a pulse reaction technique in the absence of gas phase oxygen. Methane pulse reactions demonstrate that the methane oxidation mechanism changes as the nickel oxidation state changes over Ni/TiO$_2$. CH$_4$ is efficiently oxidized into CO and H$_2$ via a direct oxidation mechanism when Ni/TiO$_2$ is reduced; while CH$_4$ may be converted by a non-selective oxidation process over oxidized Ni/TiO$_2$.
© 2004 Elsevier B.V. All rights reserved.

Keywords: Methane; Ni/TiO$_2$ catalyst; Hydrogen and carbon monoxide; Partial oxidation; Nickel oxidation states; TiO$_2$

1. Introduction

Many studies on partial oxidation of methane (POM) have been done and various viewpoints about it have been reported. POM has been interpreted to proceed via a two-step reaction pathway [1,2]. The complete oxidation of a part of the methane to carbon dioxide and steam occurs at first, and then comes the second step of reforming of the remaining methane with carbon dioxide and steam to syngas. However, direct partial oxidation of methane to syngas has also been suggested by Hickman and Schmidt [3]. They proposed a mechanism where methane was converted into carbon species on the catalyst surface via a catalytical pyrolysis followed by oxidation of the surface carbon and hydrogen desorption. So the mechanism of POM remains controversial. Therefore, a better understanding of the reaction mechanism and of the nature of the active catalytic sites is required.

Mallens et al. [4,5] found differences using Rh versus Pt catalysts, in the selectivity toward CO and H$_2$ during POM. These differences were attributed to the lower activation energy for methane decomposition on Rh versus that on Pt. Mallens et al. suggested that the catalyst's ability to activate methane determines (1) the product distribution and (2) the concentration of active surface species of oxygen, carbon and hydrogen. Fathi et al. [6] studied the partial oxidation of methane to syngas over platinum catalysts and proposed that the product distribution is determined by both the concentrations and the types of surface oxygen species present at the catalyst surface. Qin et al. [7] suggested that the support might also influence the concentration of adsorbed oxygen and, as a consequence, the activation of methane and the product distribution. Li et al. [8] studied the effect of gas phase O$_2$, reversibly adsorbed oxygen and oxidation state of the nickel in the Ni/Al$_2$O$_3$ catalyst on CH$_4$ decomposition and partial oxidation using transient response techniques at 700 °C. They concluded that the surface state of the catalyst affects the reaction mechanism and plays an important role in POM conversions and selectivities. Li et al. [8] also argued

* Corresponding author. Tel.: +86 5792283907; fax: +86 5792282595.
E-mail addresses: wth3907@163.com (T. Wu),
hlwan@xmu.edu.cn (H. Wan).

that direct oxidation is the major POM route, and that the in-direct oxidation mechanism cannot become dominant under their experimental conditions.

TiO$_2$ is a reducible metal oxide with several crystal structures. Titanium possesses a variety of oxidation states. Titania-supported metal catalysts have also been used for converting methane into syngas. Ruckenstein et al. [9,10] used 13.6 wt.% Ni/TiO$_2$ for POM and 1 wt.% Rh/TiO$_2$ for reforming methane with carbon dioxide to syngas. They found that the 13.6 wt.% Ni/TiO$_2$ catalyst was deactivated during the POM. Zhang et al. [11] studied the reforming methane with carbon dioxide to produce syngas over Rh catalysts supported on TiO$_2$, γ-Al$_2$O$_3$, MgO, SiO$_2$ and La$_2$O$_3$, and found that the participation of TiO$_2$ via a strong metal–support interaction contributed to catalyst deactivation. Direct partial oxidation of the methane to syngas occurs with the proper choice of the Ru/TiO$_2$ catalyst [12] according to transient experiments using isotope-labeled molecules. Braford and Vannice [13,14] suggested that the metal–TiO$_x$ interaction promotes the catalyst activity.

It has been well known that metal–support interactions can affect both catalytic activity and stability [15,16]. TiO$_2$-supported Group VIII metal catalysts suppress carbon formation during the reforming of methane to syngas, presumably due to the decoration of metal surfaces with TiO$_x$ species. The TiO$_x$ presence destroys the large ensembles of metal atoms that serve as active sites for carbon deposition [17,18]. Interfacial metal–support sites may promote catalyst activity [19]. Reactions on Pt/TiO$_x$ catalysts have supported this hypothesis [20]. Titania-supported nickel catalysts are more active in carbon monoxide hydrogenation than silica- or alumina-supported catalysts [21]. Suppression of hydrogen and carbon monoxide adsorption on TiO$_2$-supported metals has been observed and attributed to the strong interaction between metal and titania by Moon and co-workers [22].

The present work concerns the performance of Ni/TiO$_2$ catalysts for POM and methane activation mechanism over the catalyst. A key question remaining in POM is that whether the oxygen initiating the reaction is directly from the metal oxide (NiO) lattice or from the support TiO$_2$. This question was pursued by conventional pulse experiments and catalytic activity tests. The influence of temperature and time on stream on the catalytic performance was also investigated. Special attention was given to the correlation between the nickel oxidation states and the methane activation mechanism over the Ni/TiO$_2$ catalyst.

2. Experimental

2.1. Catalyst preparation

The supported nickel catalyst Ni/TiO$_2$ was prepared by impregnating TiO$_2$ (John Matthey Chemicals Limited, 70 m^2/g 60–80 mesh) with an aqueous solution of 0.1 M Ni(NO$_3$)$_2$·6H$_2$O. This was followed by drying overnight at 110 °C and calcination in air at 700 °C for 6 h. The nickel loading was 8 wt.%.

2.2. Reactivity test of catalyst

Catalytic performance tests were carried out in a fixed tubular quartz micro-reactor (200 mm length, 6 mm i.d.). A 500 mg catalyst sample was used for all runs. The reactor system was purged first with nitrogen for 0.5 h, and then the catalyst was reduced at 700 °C under pure hydrogen (10 mL/min) for 1 h. The reactant (CH$_4$/O$_2$ (2/1)) was then introduced to the reactor. Analyses of reactant/product mixtures were achieved by a gas chromatograph (model 103G) with a TC detector. A carbon sieve TDX-01 (packed column, 2 m length, 4 mm i.d.) column was used in order to separate hydrogen, carbon monoxide, carbon dioxide, oxygen and methane. The amount of carbon deposited on the catalyst was determined by TG analysis.

2.3. Temperature-programmed reductions (TPR) and pulse reactions

TPR and pulse reaction experiments were carried out in a fixed-bed tubular quartz micro-reactor with an inner diameter of 3 mm and a length of 18 cm. Hundred milligrams catalyst sample was used in each run. An on-line Balzer quadrupole mass spectrometer (QMS 200) continuously monitored the reactor effluent, which might contain hydrogen ($m/z = 2$), He ($m/z = 4$), methane ($m/z = 15$ or 16), water ($m/z = 18$), carbon monoxide or nitrogen ($m/z = 28$), oxygen ($m/z = 32$) and carbon dioxide ($m/z = 44$). High purity helium was used as carrier gas.

For the TPR experiment the fresh catalyst was first pretreated in air at 700 °C for 1 h and then cooled to room temperature under a helium flow. Then, the helium flow was replaced by a flow of 3% (V) hydrogen in nitrogen (30 mL/min). After the concentration of effluent was stabilized, the temperature was ramped at a rate of 15 °C/min to 1000 °C. For the used catalyst, a helium flow was introduced for 20 min, and the catalyst was cooled to room temperature. Then the flow was switched to a 3% H$_2$/N$_2$ mixture. Temperature was then increased at a rate of 15 °C/min to 1000 °C.

The pulse reaction experiments were performed at 700 °C. A gas pulse containing 1 mL CH$_4$/Ar (1/20) was injected through a six-port valve into a helium carrier gas flow, which continuously flowed through the reactor during the experiments. An unreduced Ni/TiO$_2$ catalyst sample was kept under a helium flow at 700 °C for 30 min before methane was pulsed. While a reduced catalyst sample was treated under pure hydrogen (10 mL/min) at 700 °C for 30 min before the pulse reaction.

2.4. X-ray diffraction (XRD) and nickel dispersions of Ni/TiO$_2$

XRD patterns were obtained with a Philips PW 1840 powder diffractometer. Co Kα radiation was employed, covering

Table 1
Partial oxidation of methane to syngas over 8 wt.% Ni/TiO$_2$

Temperature (°C)	CH$_4$ conversion (%)	Selectivity		H$_2$/CO (mole ratio)
		H$_2$ (%)	CO (%)	
300	–	–	–	–
400	–	–	–	–
500	58.9	74.3	47.9	2.84
600	69.5	87.4	55.0	2.81
700	76.6	93.5	74.6	2.13
800	86.3	99.7	88.2	2.09

Reaction conditions: CH$_4$/O$_2$ = 2, GHSV = 1.5 × 10^5 h^{-1}, 1 atm.

2θ between 20° and 60°. Nickel dispersion of the catalyst was measured by hydrogen chemisorption at room temperature. The percentage dispersion of nickel metal was calculated assuming the H/Ni atomic ratio of 1 [23].

3. Results

3.1. Activity of Ni/TiO$_2$ catalysts in POM

POM was tested over Ni/TiO$_2$ catalyst at temperatures from 300 to 800 °C. Table 1 showed that temperature affected the reactivity of Ni/TiO$_2$ significantly. Below 500 °C, Ni/TiO$_2$ exhibited no activity. At 500 °C, both methane conversion and selectivity to carbon monoxide were very low. However, selectivity to hydrogen was higher than that to carbon monoxide. The catalyst showed higher activity at 700 and 800 °C.

3.2. Effect of time on stream

To investigate the catalyst durability, endurance tests were carried out at 700 °C and under atmospheric pressure, CH$_4$/O$_2$ = 2/1, and GHSV = 1.5 × 10^5 h^{-1}. Catalytic performance as a function of time on stream over the Ni/TiO$_2$ catalyst is plotted in Fig. 1. Rapid deactivation was observed after the reaction was started. Methane conversion decreased from an initial value of 76% to 43% after 20 h of reaction, while CO selectivity reduced from 74% to 40% and H$_2$ selectivity from 93% to 50%.

3.3. The temperature-programmed reductions (TPR) of Ni/TiO$_2$

The nickel oxidation state in Ni/TiO$_2$ was investigated by means of TPR. Both fresh catalyst and catalysts, which had been subjected to the POM reactions, were examined with TPR in a flow of 3% (V) hydrogen in nitrogen, as presented in Fig. 2 a and b. At least three reduction peaks for fresh Ni/TiO$_2$ can be observed at temperatures of 280, 390 and 640 °C, respectively (Fig. 2a). Unsupported NiO is reduced at about 280 °C [24]. Therefore, the small peak between 250 and 300 °C in the fresh catalyst is assigned to the reduction of bulk NiO which does not interact with titania. The
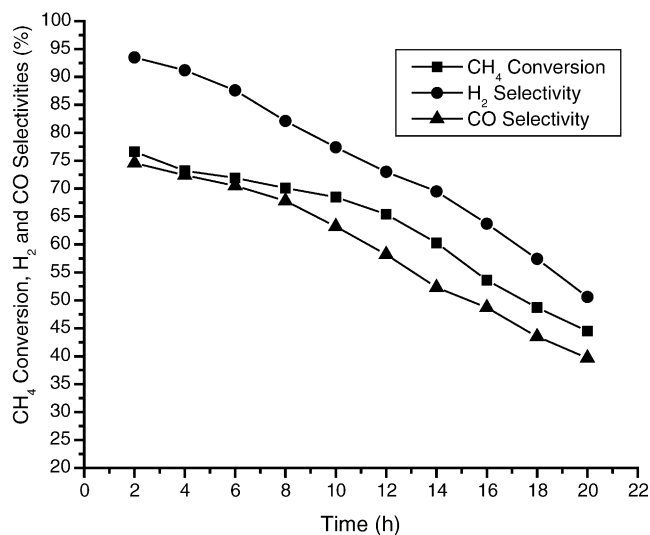

Fig. 1. Activity vs. reaction time for the POM reaction over 8 wt.% Ni/TiO$_2$ catalyst.
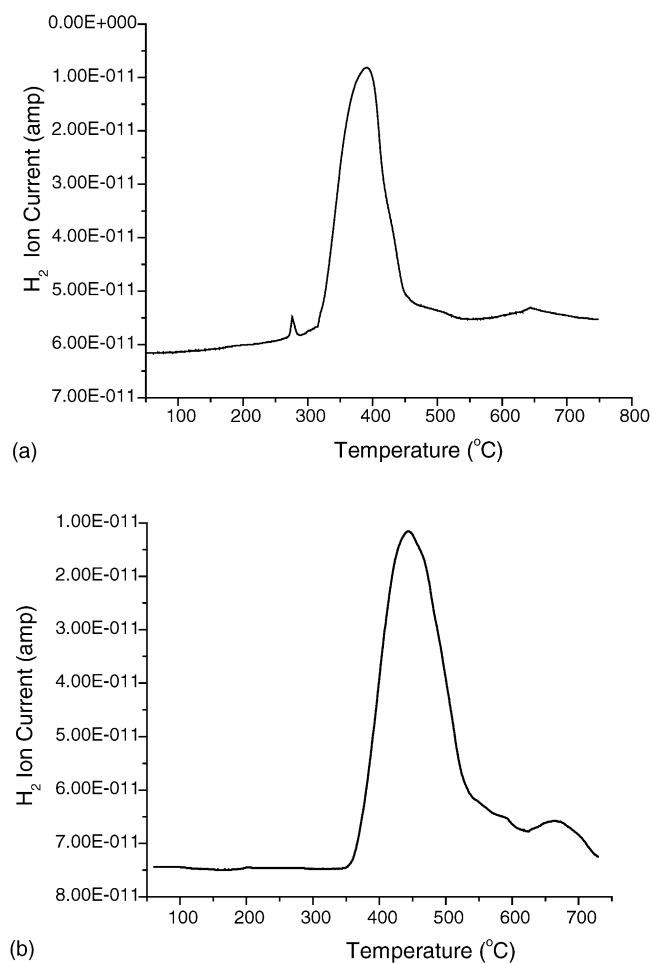

(a)

(b)

Fig. 2. Temperature-programmed reduction (TPR) profiles of: (a) fresh 8 wt.% Ni/TiO$_2$ and (b) 8 wt.% Ni/TiO$_2$ after catalyzing the POM reaction for 2 h at 700 °C.
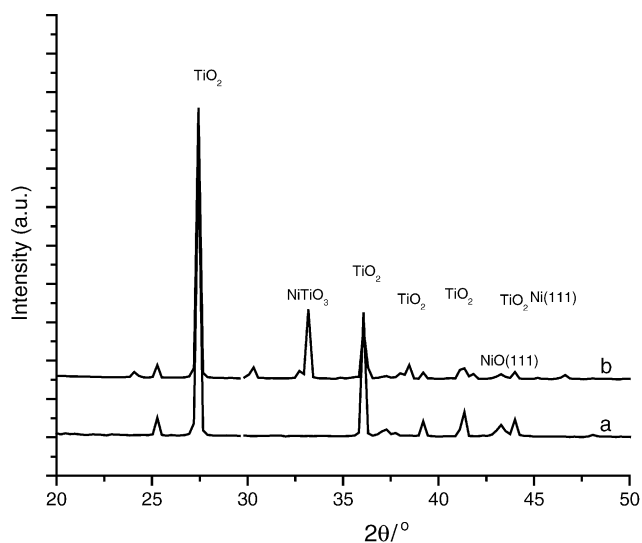
Fig. 3. XRD patterns of: (a) fresh 8 wt.% Ni/TiO$_2$ and (b) 8 wt.% Ni/TiO$_2$ after the POM reaction for 20 h at 700 °C.

higher temperature peak (390 °C) is assigned to the NiO that has significant interaction with titania (NiO–TiO$_2$ interaction species). The peak between 550 and 700 °C, is assigned to bulk NiTiO$_3$ [25].

Two peaks were detected from Ni/TiO$_2$ by TPR after POM (Fig. 2b). The peak located at 445 °C is due to the NiO–TiO$_2$ interacting species while the reduction peak at 660 °C is assigned to bulk NiTiO$_3$. Thus, oxidized nickel exists after POM on Ni/TiO$_2$. A strong interaction between NiO and TiO$_2$ also occurs during POM (Fig. 2b).

3.4. XRD patterns of Ni/TiO$_2$

The XRD patterns of 8 wt.% Ni/TiO$_2$ catalysts are shown in Fig. 3. The XRD patterns of NiO are found in addition to the diffraction peaks of rutile for fresh Ni/TiO$_2$ (Fig. 3a). NiO peaks become weak and new diffraction peaks characteristic of NiTiO$_3$ emerge after the catalyst was used for the POM for 20 h; only very tiny Ni peak is found (Fig. 3b).
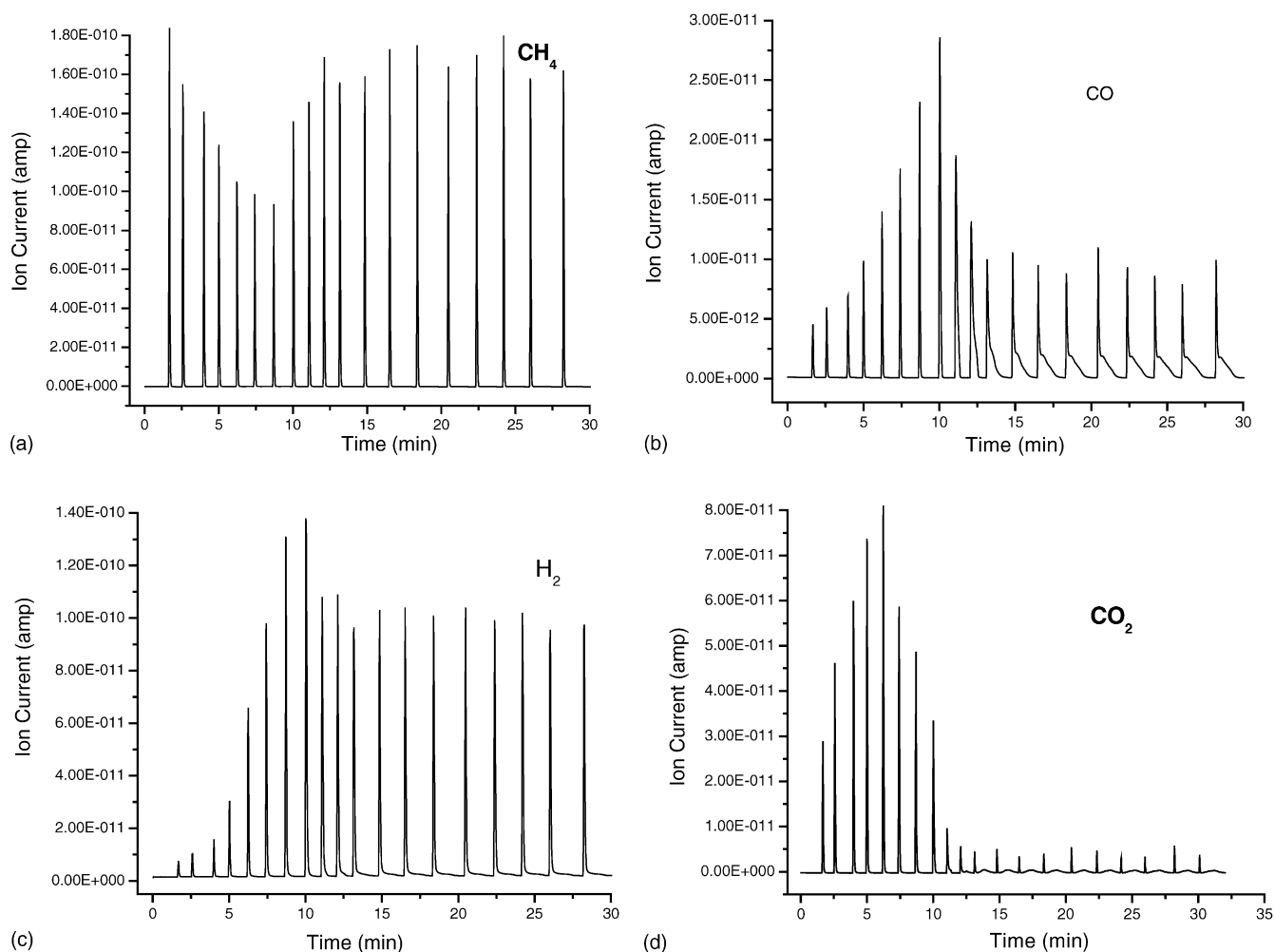

Fig. 4. Effluent gases from methane (CH$_4$/Ar, 1/20 mole ratio) pulsing experiments at 700 °C over 8 wt.% Ni/TiO$_2$ oxidized in air at 700 °C for 6 h: (a) methane, (b) carbon monoxide, (c) hydrogen and (d) carbon dioxide.

3.5. Interaction between methane and Ni/TiO₂

Pulse reactions were conducted over oxidized $Ni(O)/TiO_2$ without adding oxygen (Fig. 4a–d). Any methane oxidation in these experiments must be derived from oxygen originating from NiO and/or TiO_2 in the catalyst system. Methane diluted in argon ($CH_4/Ar = 1/20$) was pulsed (1 mL gas) over unreduced Ni/TiO₂ at 700 °C. Fig. 4a–d shows typical pulse reaction results. During the first pulse, small amounts of carbon dioxide, hydrogen and carbon monoxide were detected by MS. Thus, the surface oxygen present on the catalyst was responsible for the formation of both carbon monoxide and carbon dioxide, for there is no oxygen in the feed gas and the catalyst was not pre-reduced. Methane conversions increased over the first seven pulses, and then decreased. The yield of carbon monoxide increased from the first to the eighth pulse, then decreased. Substantial tailing of the carbon monoxide peaks was observed from the ninth pulse, and the length of the tailing increased thereafter as the pulse number increased. The carbon dioxide yield increased sharply over the first five pulses, and then decreased rapidly (Fig. 4d). After the ninth pulse, only a small amount of carbon dioxide was detected. After the 11th pulse the carbon dioxide peaks exhibited tailing. The hydrogen evolution pattern was similar to that of carbon monoxide.

Fig. 5a–d presents the results of the methane pulsing over the 8 wt.% Ni/TiO₂ catalyst, which had been reduced at 700 °C in hydrogen for 1 h. Almost all of the methane was converted during the first pulse. Methane conversion decreased rapidly with subsequent pulsing. The yields of carbon monoxide, hydrogen and carbon dioxide were highest from the first pulse, and decreased with the sequent pulses. Among the three products, carbon dioxide decreased most sharply. Only a trace of carbon dioxide was detected after the second pulse. The carbon monoxide and hydrogen peaks were found to exhibit more remarkable tailing, while no peak tailing was found for carbon dioxide.
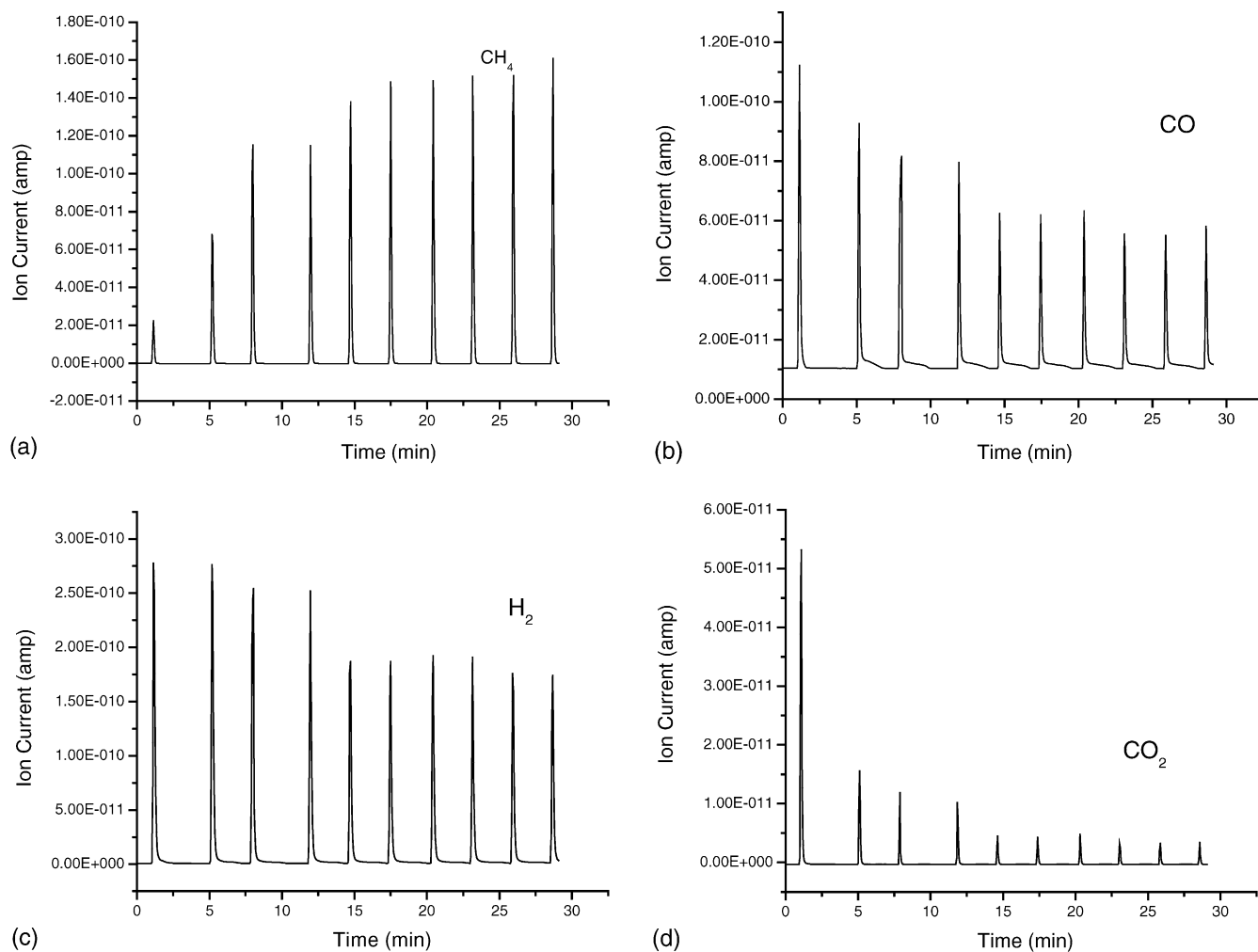

Fig. 5. Effluent gases from methane (CH₄/Ar, 1/20 mole ratio) pulsing experiments at 700 °C over 8 wt.% Ni/TiO₂ reduced in hydrogen, at 700 °C for 1 h: (a) methane, (b) carbon monoxide, (c) hydrogen and (d) carbon dioxide.

4. Discussion

4.1. Deactivation of Ni/TiO$_2$ during POM

Serious deactivation was observed for the 8 wt.% Ni/TiO$_2$ catalyst during POM. This could be mainly due to SMSI and solid-state reactions. Ruckenstein and Hu [10] observed a relatively small initial yield of carbon monoxide, which then decreased with time, during their research on POM by using a 13.6 wt.% Ni/TiO$_2$ catalyst. They attributed it to a strong interaction between TiO$_x$ and Ni during reduction in which TiO$_x$ partially migrated onto the Ni surface. The investigation we have done under the similar conditions to theirs. Both of the two studies employed the Ni/TiO$_2$ catalyst and the reactions were examined at 700 °C. Thus, SMSI may be one of the reasons for the deactivation of 8 wt.% Ni/TiO$_2$ catalyst in this work. SMSI can affect both catalyst activity and stability [15,16]. TiO$_2$-supported Group VIII metal catalysts suppress carbon formation during the reforming of methane to syngas, presumably due to the decoration of metal surfaces with TiO$_x$ species. Suppression of hydrogen and carbon monoxide adsorption on TiO$_2$-supported metals has also been observed and attributed to the strong interaction between metal and titania by Moon and co-workers [22]. But, there is a major difference between the two studies. Ruckenstein and Hu attributed carbon deposition to the decay of overall catalytic activity for syngas production over a 50 h period. However, we observed no obvious carbon deposit on the 8 wt.% Ni/TiO$_2$ catalyst after the reaction for 20 h. The difference may be due to the different nickel loadings and reaction conditions. So, carbon deposit could be excluded from the reason for the deactivation of the catalyst in this work.
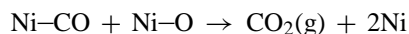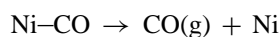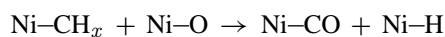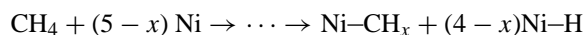
The 8 wt.% Ni/TiO$_2$ catalyst took on a color of light yellow after 20 h on stream in POM. This is the color of NiTiO$_3$, suggesting that NiTiO$_3$ was formed during POM. XRD results proved the existence of NiTiO$_3$ and NiO in the catalyst after the POM (Fig. 3). Due to the local hot spots in the catalyst bed that can exceed 1000 °C, NiO and TiO$_2$ may react in the solid phase in the presence of oxygen gas to form NiTiO$_3$ (NiO + TiO$_2$ → NiTiO$_3$) which is inert to POM. The TPR results also demonstrated the formation of NiO and NiTiO$_3$ during POM. This is in accord with the report written by Rao et al. [26] that NiTiO$_3$ was formed when Ni/TiO$_2$ was calcined above 500 °C. Besides, de Bokx et al. [27] also reported the formation of NiTiO$_3$ at the temperature of 750 °C, which was accompanied by a color change from gray to light yellow or bright yellow. So NiTiO$_3$ and NiO were formed indeed during POM. Since both of them are inactive for POM, the formation of NiTiO$_3$ and NiO is thought to be another cause for the catalyst deactivation.

4.2. Effects of nickel oxidation states on methane oxidation mechanism over Ni/TiO$_2$

Different surface metal oxidation states can result in different mechanisms [4,5,7]. CH$_4$ pulse experiments provide some mechanistic insight of methane oxidation over Ni/TiO$_2$ under different nickel oxidation states.

During the first pulse over unreduced Ni/TiO$_2$, CH$_4$ was negatively converted due to the absence of active Ni^0 sites. Only traces of CO, H$_2$ and CO$_2$ were detected. As the methane pulsing over the unreduced Ni/TiO$_2$ was continued, the methane conversion increased. This is due to the reduction of NiO to Ni^0 on the surface. Since there was no oxygen in the feed, the formation of carbon monoxide and carbon dioxide demonstrates that the catalyst itself supplies the oxygen. Surface OH groups and/or NiO lattice oxygen (O^{2-}) and/or oxygen from the TiO$_2$ support participated in the oxidation of methane to CO$_x$. It is consistent with the previous conclusion drawn by Buyevskaya et al. [28] that surface OH groups of the support were involved in the conversion of CH$_x$ to carbon monoxide. Pure TiO$_2$ did not catalyze methane conversion at 700 °C. Therefore, reduced nickel sites are required for the reaction between surface OH groups and/or low coordination oxygen of the TiO$_2$ support and methane to form CO$_x$. NiO appears to be responsible for the formation of carbon dioxide and water observed in the first five pulses. Haber [29] pointed out that total oxidation of hydrocarbons is often observed over transition metal oxides even in the absence of gaseous oxygen. Hence, a redox reaction between methane and nickel oxide (CH$_4$ + 4NiO → CO$_2$ + 2H$_2$O + 4Ni^0) on the oxidized catalysts appears reasonable. According to the reaction above, it was estimated that 15 pulses of methane were sufficient to reduce all NiO contained in 8 wt.% Ni/TiO$_2$ catalyst. However, the Ni dispersion of the fresh catalyst was only 10.3%. Thus, NiO on the surface was completely reduced to metallic nickel after the first five pulses of methane over the fresh catalyst. Both unreduced and reduced Ni/TiO$_2$ catalysts were active for methane oxidation, indicating that methane C−H bond dissociation was indeed a key step for carbon monoxide formation. This suggests that carbon monoxide formation proceeds via CH$_x$ ($x = 0$–3) species produced by methane dissociation at Ni^0 sites. During the first five pulses of methane over the oxidized catalysts, three types of reactions occurred: (1) complete oxidation to carbon dioxide over nickel oxide, (2) partial oxidation to carbon monoxide and (3) decomposition to surface carbon species over the resulting metallic nickel:

$$CH_4 + 4NiO \rightarrow CO_2 + 2H_2O + 4Ni^0$$

$$CH_4 + (5-x)\,Ni \rightarrow \cdots \rightarrow Ni\text{–}CH_x + (4-x)Ni\text{–}H$$

$$Ni\text{–}CH_x + Ni\text{–}O \rightarrow Ni\text{–}CO + Ni\text{–}H$$

$$Ni\text{–}CO \rightarrow CO(g) + Ni$$

$$Ni\text{–}CO + Ni\text{–}O \rightarrow CO_2(g) + 2Ni$$

After reduction of Ni/TiO$_2$ at 700 °C for 1 h, the surface oxygen concentration at active Ni sites was very low. Therefore, the TiO$_2$ support was the main source of oxygen. Hydrogen, carbon monoxide, carbon dioxide and water

were observed in the gas phase, when methane was pulsed over freshly reduced Ni/TiO$_2$. Methane conversion decreased upon continued pulsing. Two factors could contribute to the above phenomenon: (1) the amount of oxygen species reaching nickel sites decreased and (2) metallic sites might become increasingly poisoned (covered) by carbon species. The methane pulse reactions reveal that lattice oxygen participates in the reaction over both unreduced and reduced catalyst. Hu and Ruckenstein also found the fact by using isotopic methods that the lattice oxygen participated in the reaction even when the gas feed contained oxygen [30].

A remarkable tailing of the carbon monoxide, hydrogen and carbon dioxide peaks was observed from the ninth pulse onward during oxygen-free methane pulsing over unreduced Ni/TiO$_2$. These peaks tailed for 1–3 min before reaching background level, while CH$_4$ peaks lasted only 5–8 s. Furthermore, separate pulsing of carbon monoxide, carbon dioxide or hydrogen over the Ni/TiO$_2$ catalyst bed (either reduced or oxidized) did not give any tailing. Only sharp peaks were observed. These observations imply that the rate-determining step in the syngas formation involves a carbon species reacting with oxygen species over the catalyst. The side reaction producing carbon dioxide from carbon monoxide and oxygen was fast. So the tailing of carbon dioxide peaks observed was due to the original carbon monoxide tailing. This was confirmed by observing sharp carbon dioxide peaks upon pulsing carbon monoxide over the catalyst. Thus, the reaction between CH$_x$ and surface oxygen species could be the rate-determining step in the syngas formation over Ni/TiO$_2$.

Carbon monoxide and hydrogen exhibited longer tailing responses during the pulsing of CH$_4$/Ar over reduced Ni/TiO$_2$ (Fig. 5a–d). This indicates that CH$_x$ species are present on the reduced catalyst. As CH$_x$ species are not present on oxidized (NiO/TiO$_2$) catalyst samples, Ni^0 is responsible for their formation from methane. The carbon monoxide peaks formed after the second CH$_4$/Ar pulse over reduced Ni/TiO$_2$ exhibited long tailings (Fig. 5b). This observation could result from the desorption of carbon monoxide formed in the earlier pulses or carbon monoxide formation by reactions between surface CH$_x$ and oxygen species. Since tailing was not found for carbon dioxide, carbon monoxide desorption is ruled out and surface reaction between the CH$_x$ and the oxygen species is favored. When carbon monoxide is pulsed over the reduced catalyst, sharp peaks are obtained. Consequently, the reaction over the reduced Ni/TiO$_2$ catalyst takes place via the direct surface oxidation mechanism, in which the adsorbed CH$_x$ and oxygen species are involved.

Methane pulse reactions demonstrate that the mechanism of methane oxidation changes at different stages as the oxidation state of nickel changes. Methane can be oxidized by oxygen in NiO or by active oxygen within the TiO$_2$ support via the non-selective oxidation mechanism over oxidized Ni/TiO$_2$ which may contain NiO and NiTiO$_3$. Methane is efficiently activated via a direct oxidation mechanism only when the nickel is reduced to Ni^0 or when its surface oxygen species concentration is very low. This produces car-

bon monoxide and hydrogen, via the direct surface oxidation mechanism in which adsorbed methane and oxygen species react with each other [31]. The catalytic performance of Ni/TiO$_2$ at 700 °C under atmospheric pressure, CH$_4$/O$_2$ = 2/1, GHSV = 1.5 × 10^5 h^{-1} deactivated quickly after the reaction was started (Fig. 1). Methane conversion decreased from an initial value of 76% to 43% after 20 h of reaction, while the selectivities to CO and H$_2$ reduced significantly from 74% to 40% and 93% to 50%, respectively. These results also support direct surface oxidation with reduced Ni/TiO$_2$ and non-selective oxidation over oxidized Ni/TiO$_2$ with formation of NiO and NiTiO$_3$, in agreement with methane oxidation mechanisms proposed based on the pulse reaction studies.

5. Conclusions

The 8 wt.% Ni/TiO$_2$ catalyst was seriously deactivated during POM, which could mainly be due to: (1) SMSI between nickel oxides and titania and (2) the formation of NiO and NiTiO$_3$ in Ni/TiO$_2$. No substantial buildup of surface carbonaceous species occurs and thus surface carbon is excluded from the cause of the loss of catalyst activity. Methane pulse reactions indicate that the mechanism of methane oxidation changes at different stages as nickel oxidation state changes. Methane is oxidized by lattice oxygen in NiO or by active oxygen in the TiO$_2$ support via the non-selective mechanism over oxidized Ni/TiO$_2$, while it is efficiently converted into carbon monoxide and hydrogen via a direct oxidation mechanism when Ni/TiO$_2$ is reduced or partially reduced.

Acknowledgements

References

[1] M. Prettre, Ch. Eichner, M. Perrin, Trans. Faraday Soc. 43 (1946) 335.
[2] D. Dissanayake, M.P. Rosynek, K.C.C. Kharas, J.H. Lunsford, J. Catal. 132 (1991) 117.
[3] D.A. Hickman, L.D. Schmidt, Science 259 (1993) 343.
[4] J.E.P. Mallens, J.H.B.J. Hoebink, G.B. Marin, J. Catal. 167 (1997) 43.
[5] J.E.P. Mallens, J.H.B.J. Hoebink, G.B. Marin, Catal. Lett. 33 (1995) 291.
[6] M. Fathi, F. Monnet, Y. Schuurman, A. Holmen, C. Mirodatos, J. Catal. 190 (2000) 439.
[7] D. Qin, J. Lapszewicz, X. Jiang, J. Catal. 159 (1996) 140.
[8] C. Li, C. Yu, S. Shen, Catal. Lett. 67 (2–4) (2000) 139.
[9] E. Ruckenstein, H.Y. Wang, J. Catal. 187 (1999) 151.

[10] E. Ruckenstein, Y.H. Hu, J. Catal. 162 (1996) 230.

[11] Z.L. Zhang, V.A. Tsipouriari, A.M. Efstathiou, X.E. Verykios, J. Catal. 158 (1996) 51.

[12] C. Elmasides, D.I. Kondarides, W. Grunert, X.E. Verykios, J. Phys. Chem. B 103 (1999) 5227.

[13] M.C.J. Braford, M.A. Vannice, Catal. Today 50 (1999) 87.

[14] M.C.J. Braford, M.A. Vannice, J. Catal. 183 (1998) 69.

[15] M.C. Braford, M.A. Vannice, Appl. Catal. A 142 (1996) 73.

[16] A. Erdohelyi, J. Cserenyi, F. Solymosi, J. Catal. 141 (1993) 287.

[17] M.C.J. Braford, M.A. Vannice, J. Catal. 173 (1998) 157.

[18] A. Erdoehelyi, J. Cserenyi, E. Papp, F. Solymosi, Appl. Catal. A 108 (1994) 205.

[19] A.M. Efstathiou, A. Kladi, V.A. Tsipouriari, X.E. Verykios, J. Catal. 158 (1996) 64.

[20] M.C.J. Braford, M.A. Vannice, Catal. Lett. 48 (1997) 31.

[21] M.A. Vannice, R.L. Garten, J. Catal. 56 (1979) 236.

[22] M.A. Vannice, C.C. Twu, S.H. Moon, J. Catal. 79 (1983) 70.

[23] C. Hoang-van, Y. Kachaya, S.J. Teichner, J.A. Dalmon, Appl. Catal. 46 (1989) 281.

[24] L. Zhang, J. Lin, Y. Chen, J. Chem. Soc., Faraday Trans. 1 88 (1992) 2075.

[25] P.S. Kumbhar, Appl. Catal. 96 (1993) 241.

[26] C.N.R. Rao, G.U. Sankar, T. Rayment, J. Mater. Chem. 1 (1991) 299.

[27] P.K. de Bokx, R.L.C. Bonne, J.W. Geus, Appl. Catal. 30 (1987) 33.

[28] O.V. Buyevskaya, D. Wolf, M. Baerns, Catal. Lett. 29 (1994) 249.

[29] J. Haber, in: J.P. Bonnelle, B. Delmon, E. Derouane (Eds.), Surface Properties and Catalysis by Non-metals, Reidel, Dordrecht, 1982.

[30] Y.H. Hu, E. Ruckenstein, J. Phys. Chem. A 102 (1998) 10568.

[31] Y.H. Hu, E. Ruckenstein, J. Phys. Chem. B 102 (1998) 230.